

Comparison of MISR and MODIS bidirectional reflectance products

CHEN Yong-mei^{1,2}, WANG Jin-di¹, LIANG Shun-lin³, WANG Dong-wei¹, MA Bin¹

1. State Key Laboratory of Remote Sensing Science, Beijing Normal University Beijing 100875, China;

2. Collage of meteorology, PLA University of Science and Technology, Jiangsu Nanjing 211101, China;

3. Department of Geography, University of Maryland, College Park, MD 20742, USA;

Abstract: The Bidirectional Reflectance Distribution Function (BRDF) of land surfaces specifies the behavior of surface directional reflectance as a function of illumination and viewing angles. The bidirectional reflectance products of the Moderate resolution Imaging Spectroradiometer (MODIS) and the Multiangle Imaging Spectroradiometer (MISR) and their BRDF model parameters products have been available respectively. Since the BRDF model parameters are inverted from limited angular observations for a given pixel, it is necessary to evaluate whether they can effectively characterize the directional reflectance in other viewing directions. In this study, we choose four kinds of land cover types to analyze the representation of MISR and MODIS BRDF model parameters, by comparing the directional reflectance extrapolated using the BRDF model parameters with the observed directional reflectance. The results show that: (1) both MODIS and MISR BRDF model parameters have better representation on directional reflectance at some viewing directions. Especially MISR BRDF model parameters have preferable representations at MODIS viewing directions; (2) the representative ability of both BRDF model parameters tends to weaken when the viewing zenith angle increases; (3) from the analysis of the observed data set shown in this paper, it seems that the representative ability of MODIS BRDF models is better near cross-principal plane than that near principal plane.

Key words: BRDF model, MISR, MODIS, model parameters, extrapolation

CLC number: TP702

Document code: A

1 INTRODUCTION

The Bidirectional Reflectance Distribution Function (BRDF) describes the directional reflectance properties of the land surface as a function of illumination and viewing angles. BRDF properties of land surfaces have been paid much more attention in advanced remote sensing data analysis and applications (Lucht *et al.*, 2000; Wanner *et al.*, 1997). The bidirectional reflectance observations and BRDF models can be used to retrieve the structural parameters of the land surface, such as LAI (Feng & Zhao, 2007). The BRDF models can be used to obtain the corrected nadir viewing reflectance from the observations with varying sun-view geometries (Leroy & Roujean, 1994; Lucht *et al.*, 2000). Most importantly, the integrated bidirectional reflectance observations allow specification of land surface albedo more exactly. So, much attention should be paid on the extrapolation ability of the existing multi-angle remote sensing observations on the BRDF character at pixel scale, and on the applicability of the BRDF model parameter products in the relative studies.

At present, the Multi-angle Imaging Spectroradiometer (MISR) and Moderate Resolution Imaging Spectroradiometer

(MODIS)'s bidirectional reflectance products, the relative BRDF model parameters and the albedo products have been available. Their BRDF model parameters products are inverted from the observations with limited viewing directions. The applicability of a BRDF product can be analyzed partially with respect to the calculation of albedo, and many validation work on MODIS albedo products have been done (Jiao *et al.*, 2005; Liang *et al.*, 2002). However, albedo may not include all of the information of the bi-directional reflectance of land surface. For example, the same albedos may correspond to different BRDF model parameters. So, learning the extrapolation ability of MISR and MODIS BRDF model parameters products at those directions without observed data is an important method to evaluate the applicability of BRDF model parameters.

To learn the extrapolation ability of MISR and MODIS BRDF model parameters products at those directions without observed data, we need many field measurements on the bidirectional reflectance of many directions and different land cover types. However, they can not be easily measured. Additionally, some bidirectional reflectances are measured in the field or from airborne instruments, with limited sampling of viewing directions and a poor spatial coverage (Bicheron & Leroy, 2000). The similarity between MISR and MODIS prod-

Received: 2008-04-28; **Accepted:** 2008-10-31

Foundation: National Natural Science Foundation of China (Grant No. 40571107, 40871163, 40640420073), and Major State Basic Research Development Program of China (No. 2007CB714407).

First author biography: CHEN Yong-mei (1983—), female, assistant. She graduated from State Key Laboratory of Remote Sensing Science, Beijing Normal University in 2008, and now works in Collage of meteorology, PLA University of Science and Technology, Nanjing.

Corresponding accthor: WANG Jin-di, E-mail: wangjd@bnu.edu.cn

ucts can help us to solve this problem. In this paper, we make use of the similarity between MISR and MODIS products to analyze the extrapolation ability of MISR and MODIS BRDF model parameter products. The spatial and spectral resolutions of MISR reflectance products and MODIS BRDF products are similar. Given the 9 MISR illumination and viewing angles, we make use of the 3 MODIS BRDF model parameters to calculate the reflectance at the corresponding 9 angles. From the comparison of the calculated 9 angles reflectances and the MISR measured 9 angles reflectances provided in its products, the extrapolation ability of MODIS BRDF parameters products can be analyzed. Similarly, we can use the MODIS reflectance products to analyze the extrapolation ability of MISR BRDF model parameters products.

2 DATA

2.1 Test sites of typical land cover types

MISR and MODIS BRDF model parameters products and their bidirectional reflectance products of the year of 2001 of the four land cover types like “Grasslands”, “Barren or sparsely vegetated”, “Evergreen needleleaf forest” and “Croplands” are used in this paper. Each land cover type includes four test sites (as shown in Table 1). The MODIS BRDF model parameters products and the bidirectional reflectance products are downloaded from ORNL DAAC (Oak Ridge National Laboratory Distributed Active Archive Center). The MISR BRDF model parameters products and the bidirectional reflectance products are provided by Dr. Fang Hongliang of University of Maryland.

Table 1 Information of each test site

Land cover types	Site Name	Longitude	Latitude
Grasslands	Sevilleta BigFoot	106.70°W	34.36°N
	Konza Prairie LTER	96.56°W	39.08°N
	Rannells Ranch (grazed)	96.53°W	39.14°N
	Sevilleta Nat Refuge-Mackenzie Flats	106.67°W	34.36°N
Barren or sparsely vegetated	La Paz	110.44°W	24.13°N
	Arabial	46.76°E	18.88°N
	Ivanpah Playa Nevada/California	115.39°W	35.55°N
	Railroad Valley Playa 2	115.70°W	38.50°N
Evergreen needleleaf forest	Sask.-1994 Harv. Jack Pine	104.66°W	53.91°N
	BOREAS NSA-Old Black Spruce	98.48°W	55.88°N
	BOREAS NSA Young Jack Pine	98.29°W	55.90°N
	Black Hills	103.65°W	44.16°N
Croplands	Bondville	88.29°W	40.01°N
	Pleasant Plains	89.88°W	39.5°N
	Walnut River Watershed	96.86°W	37.52°N
	ARM Southern Great Plains site-Lamont	97.49°W	36.61°N

2.2 Reflectance and BRDF model parameters products of MISR

The Multi-angle Imaging SpectroRadiometer (MISR) is one of the instruments onboard the National Aeronautics and Space Administration (NASA)’s Earth Observing System (EOS) Terra satellite. MISR views the sunlit Earth simultaneously in four spectral bands at nine widely spaced angles (0° , $\pm 26.1^\circ$, $\pm 45.6^\circ$, $\pm 60.0^\circ$ and $\pm 70.5^\circ$). The central wave length of the four bands are 446, 558, 672 and 867 nm (Bull *et al.*, 2005). The MISR data used in this study is the radiometrically, geometrically and atmospherically calibrated MISR Level 2 Land Surface Parameter Products. That are the MISR 9 angle reflectance products, and the BRDF model parameters products which are inverted from the 9 angle reflectance products. The spatial resolutions of the two products are 1.1km (Diner *et al.*, 1999; Wan *et al.*, 2007).

For MISR products, a modified form of the BRDF model of Rahman *et al.* (1993) is used, and is described by the following equation (Diner *et al.*, 1999; Rahman *et al.*, 1993):

$$R_{\text{model}}(-\mu, \mu_0, \phi) = r_0 \times \frac{\mu^{k-1} \mu_0^{k-1}}{(\mu + \mu_0)^{1-k}} \times \exp[bp(\Omega)] \times h(-\mu, \mu_0, \phi) \quad (1)$$

In equation (1), r_0 , k , b are three free parameters. μ and μ_0 are the cosine of the view zenith angle (θ) and sun zenith angle (ϑ). ϕ is the relative azimuth angle. The function $p(\Omega)$ is assumed to depended only on the scattering angle Ω , and here it is defined as the function of θ , ϑ and ϕ :

$$p(\Omega) = \cos \Omega = -\mu \mu_0 + (1 - \mu^2)^{1/2} \times (1 - \mu_0^2)^{1/2} \times \cos \phi \quad (2)$$

In equation (1), the function h is a factor to account for the hot spot:

$$h(-\mu, \mu_0, \phi) = 1 + \frac{1 - r_0}{1 + G(-\mu, \mu_0, \phi)} \quad (3)$$

with

$$G(-\mu, \mu_0, \phi) = \{(\mu^{-2} - 1) + (\mu_0^{-2} - 1) + 2\left[\sqrt{(\mu^{-2} - 1)(\mu_0^{-2} - 1)}\right] \cos \phi\}^{1/2} \quad (4)$$

From equation (1)—(4) we can see that, if the three parameters (r_0 , k , b) of the Rahman model are known, we can use equation (1) to calculate the reflectance of any angle (θ , ϑ , ϕ). The MISR BRDF model parameter products are the three parameters of Rahman model with the spatial resolution of 1.1km.

2.3 Reflectance and BRDF model parameters products of MODIS

MODIS is also an instrument onboard Terra. The MODIS data used in this study are the BRDF model parameters products (MOD43B1), with the spatial resolution of 1km, and the reflectance products (MOD09A1), with the spatial resolution of 500m (Schaaf *et al.*, 2002).

The operational MODIS BRDF algorithm makes use of a kernel-driven, liner BRDF model, and can be described by the following equation (Lucht *et al.*, 2000; Roujean *et al.*, 1992;

Schaaf *et al.*, 2002):

$$R(\theta, \vartheta, \phi) = f_{\text{iso}} + f_{\text{geo}} K_{\text{geo}}(\theta, \vartheta, \phi) + f_{\text{vol}} K_{\text{vol}}(\theta, \vartheta, \phi) \quad (5)$$

In equation (5), f_{iso} is the isotropic-scattering parameter. K_{geo} and K_{vol} are the geometric-optical and the volume-scattering contributions, and they are the functions of view zenith angle (θ), sun zenith angle (ϑ) and relative azimuth angle (ϕ). f_{geo} and f_{vol} are their respective weights.

MODIS scans across-track. By virtue of its wide scan, MODIS obtains the multi-angle observations mostly from the overlaps of different swaths. MODIS BRDF algorithm makes use of the registered MODIS multi-angle observations to fit the kernel-driven BRDF model and provides a global BRDF parameters products (f_{iso} , f_{geo} , f_{vol}) at 1-km resolution on a 16-day cycle. Since K_{geo} and K_{vol} are functions of θ , ϑ and ϕ . From equation (5) we can see that, if the 3 BRDF parameters (f_{iso} , f_{geo} , f_{vol}) of MODIS are known, we can use equation (5) to calculate the reflectance of any angle (θ , ϑ , ϕ). We call the process that calculates reflectance of other directions from finite observations the extrapolation process. The MODIS BRDF model parameters products are the three parameters (f_{iso} , f_{geo} , f_{vol}) of kernel-driven model at 1-km spatial resolution.

3 METHODS AND RESULTS

3.1 Correspondence of MISR and MODIS data on spatial, temporal and spectral resolution

Before analyzing MISR and MODIS data products, the correspondence of these two products on spatial, temporal and spectral resolution should be made.

ORNL DAAC provides the MODIS data products of the pixel corresponding to the typical test sites, and the longitude and latitude information of these sites. According to the longitude and latitude of each site, we use GCTP (General Cartographic Transformation Package Software) to find the MISR pixel corresponding to the site. The spatial resolution is 1.1km and 1km for MISR reflectance products and MODIS BRDF model parameters products respectively. So, for one pixel, their spatial resolution can be approximately taken as the same. The spatial resolution of the MODIS reflectance products (MOD09A1) used in this study is 500m (Schaaf *et al.*, 2002), while the resolution of MISR BRDF model parameters is 1.1km. One MISR BRDF model parameters products pixel corresponds to about 4 MOD09A1 pixels. Since the MOD09A1 product is the best one of 8 days, the imaging time and the illumination and viewing angles of the 4 MOD09A1 pixels may be different. Supposing that the observing object is uniform at the MISR pixel scale, and the reflectance of the pixel does not change greatly, the reflectances of the 4 MOD09A1 pixels can be taken as 4 reflectances of a MISR pixel from 4 different illumination and viewing directions. In this way, we can construct the correspondence between MISR BRDF model parameters products and MODIS reflectance products.

MISR views the sunlit earth simultaneously at 9 angles, and the MISR BRDF model parameters products are built from the

9 instantaneous observations. While the MODIS BRDF algorithm makes use of a semi-empirical kernel-driven bidirectional reflectance model (AMBRALS) and multi-date and multi-angle observations to provide global BRDF products every 16 days. MODIS provides reflectance product (MOD09A1) every 8 days. So, in this study, we analyze the extrapolation ability of MODIS BRDF products on every 16 days. For example, the MISR reflectance with the DOY (day of year) between 1 and 16 is used to analyze the extrapolation ability of MODIS BRDF model parameters products with the DOY of 16. Similarly, we analyze the extrapolation ability of MISR BRDF model parameters products on every 8 days.

MISR and the first 4 bands of MODIS have similar spectral wavelength range in the visible and near infrared bands (Jin *et al.*, 2002). As shown in Table 2, MISR bands 1, 2, 3, 4 correspond to MODIS bands 3, 4, 1, 2 respectively.

Table 2 Correspondence between MISR and MODIS bands

Band name	MODIS		MISR	
	Band number	Wavelength/nm	Band number	Wavelength/nm
Blue	3	459—479	1	425—467
Green	4	545—565	2	543—572
Red	1	620—670	3	661—683
Near infrared	2	841—876	4	847—886

3.2 Comparison of MISR and MODIS BRDF model parameters products

For the pixel of each test site, extract the MISR and MODIS BRDF model parameters products, the multi-angle reflectance products, and the corresponding sun-view geometry (sun zenith angle, view zenith angle, relative azimuth angle). Given the 9 MISR illumination and viewing angles, we use the 3 MODIS kernel-driven BRDF model parameters to calculate the reflectance at the corresponding 9 angles. Then, compare the calculated 9 angle reflectance and MISR 9 angle reflectance products, using the R-square (R^2) and Residual standard error (RSE) to characterize the extrapolation ability of MODIS BRDF model parameters products at the 9 MISR view geometries. In the same way, given the 4 MODIS reflectance products (MOD09A1) and the illumination and viewing angles, we use the 3 MISR BRDF model parameters to calculate the reflectance at the corresponding 4 angles. From the comparison of the calculated reflectance and the MODIS reflectance products, the extrapolation ability of MISR BRDF model parameters products at the 4 MODIS view geometries can be analyzed.

3.2.1 Variability of the extrapolation ability of MISR and MODIS BRDF model parameters products with viewing zenith angles

In order to analyze the extrapolation ability of MISR and MODIS BRDF model parameters products and their variability with viewing zenith angles, we divide the MISR and MODIS reflectance products into two groups according to the viewing zenith angles: ① viewing zenith angle $< 30^\circ$; ② viewing zenith angle $> 30^\circ$.

Fig. 1 and Fig. 2 are the comparison of the extrapolation ability of the two BRDF model parameters products. The red points represent the viewing zenith angle 30° ; the black points represent the viewing zenith angle $>30^\circ$.

In order to analyze the variability of the extrapolation ability of the two BRDF model parameters products with viewing zenith angles quantitatively, we calculate the R^2 and RSE for the large and small view zenith angles separately (shown in Table 3 and Table 4). For “Grasslands” and “Croplands”, the view zenith angles of MODIS reflectance product are all less than 30° , so we did not do the comparison for them in Table 4.

From Fig. 1 we can see that the bidirectional reflectance calculated using MODIS BRDF model parameters products fit the MISR bidirectional reflectance better when the viewing zenith angle 30° (red points) than that when the viewing zenith angle $>30^\circ$ (black points). From Table 3 we can also see that when the view zenith angles are smaller, the R^2 increase and the RSE decrease.

MISR can obtain the observing reflectance of the same target from 9 angles. Comparing with the observation mode of MODIS, MISR gains the advantage over MODIS on obtaining

more directional observations, especially on the observations at large view zenith angles. So, from Fig. 2 and Table 4 we can see that: the bidirectional reflectance calculated using MISR BRDF model parameters products fit the MODIS bidirectional reflectance more preferably. Although the fitting becomes disperse when the view zenith angle increase, the MISR BRDF model parameters products show preferable extrapolation ability.

3.2.2 Variability of the extrapolation ability of MODIS BRDF model parameters products with relative azimuth angles

In order to analyze the extrapolation ability of MISR and MODIS BRDF model parameters products and their variability with relative azimuth angles, we divided the MISR and MODIS reflectance products into 4 groups according to the relative azimuth angles: ① relative azimuth angle $\in (0^\circ, 30^\circ)$; ② relative azimuth angle $\in (150^\circ, 180^\circ)$; ③ relative azimuth angle $\in (60^\circ, 120^\circ)$; ④ the other angles.

Fig. 3 is the comparison result of the extrapolated directional reflectance calculated using the MODIS BRDF model parameters products and the MISR 9 angle reflectance products. The black points represent group ①, the blue points represent group ②, the green points represent group ③, and the red

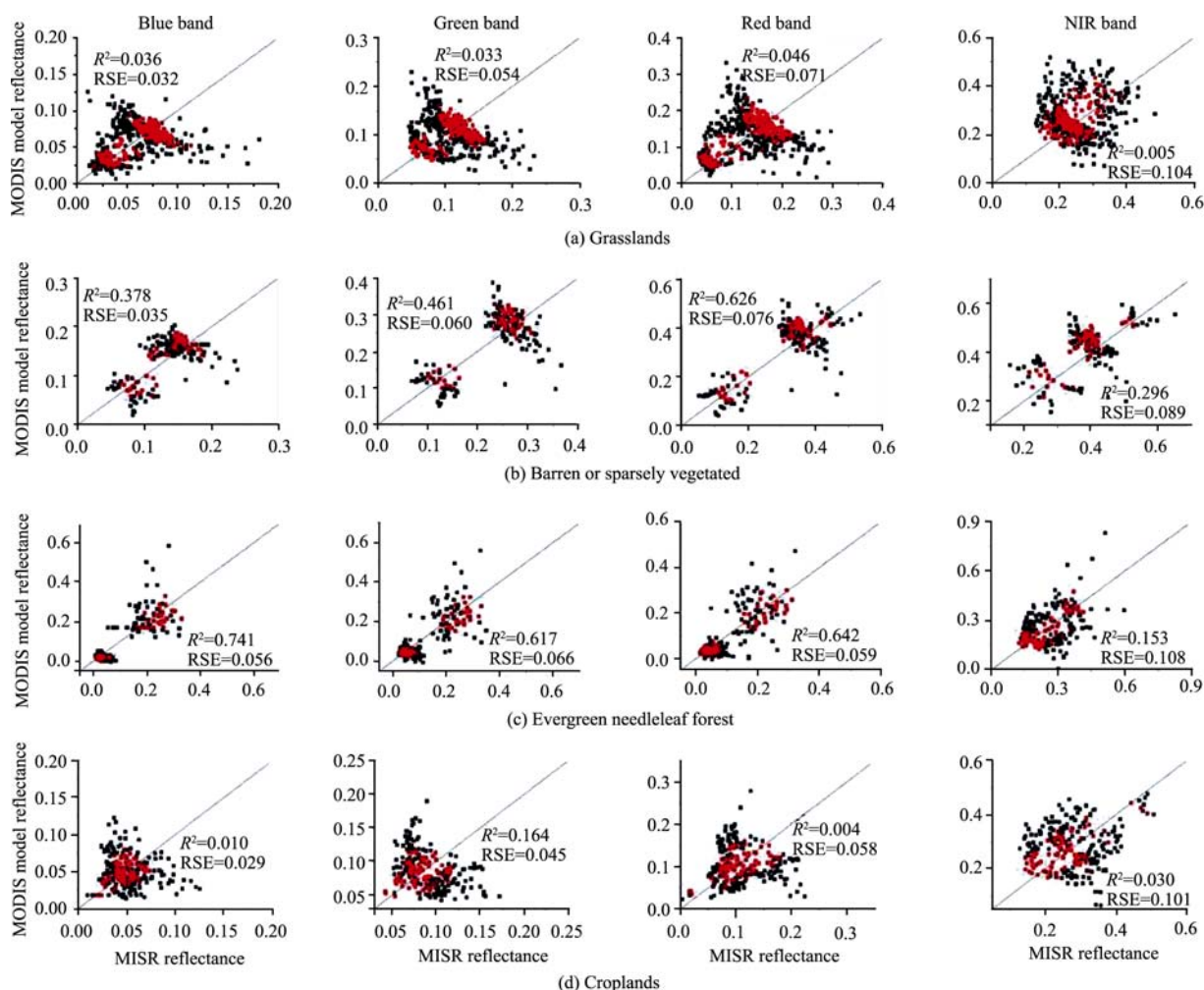


Fig. 1 Fittings of the MODIS BRDF model parameters products with the MISR 9 angle reflectance products. The red points represent the view zenith angle 30° ; the black points represent the view zenith angle $>30^\circ$. The X coordinate is the MISR reflectance products and the Y coordinate is the reflectance calculated using the MODIS BRDF model parameters products.

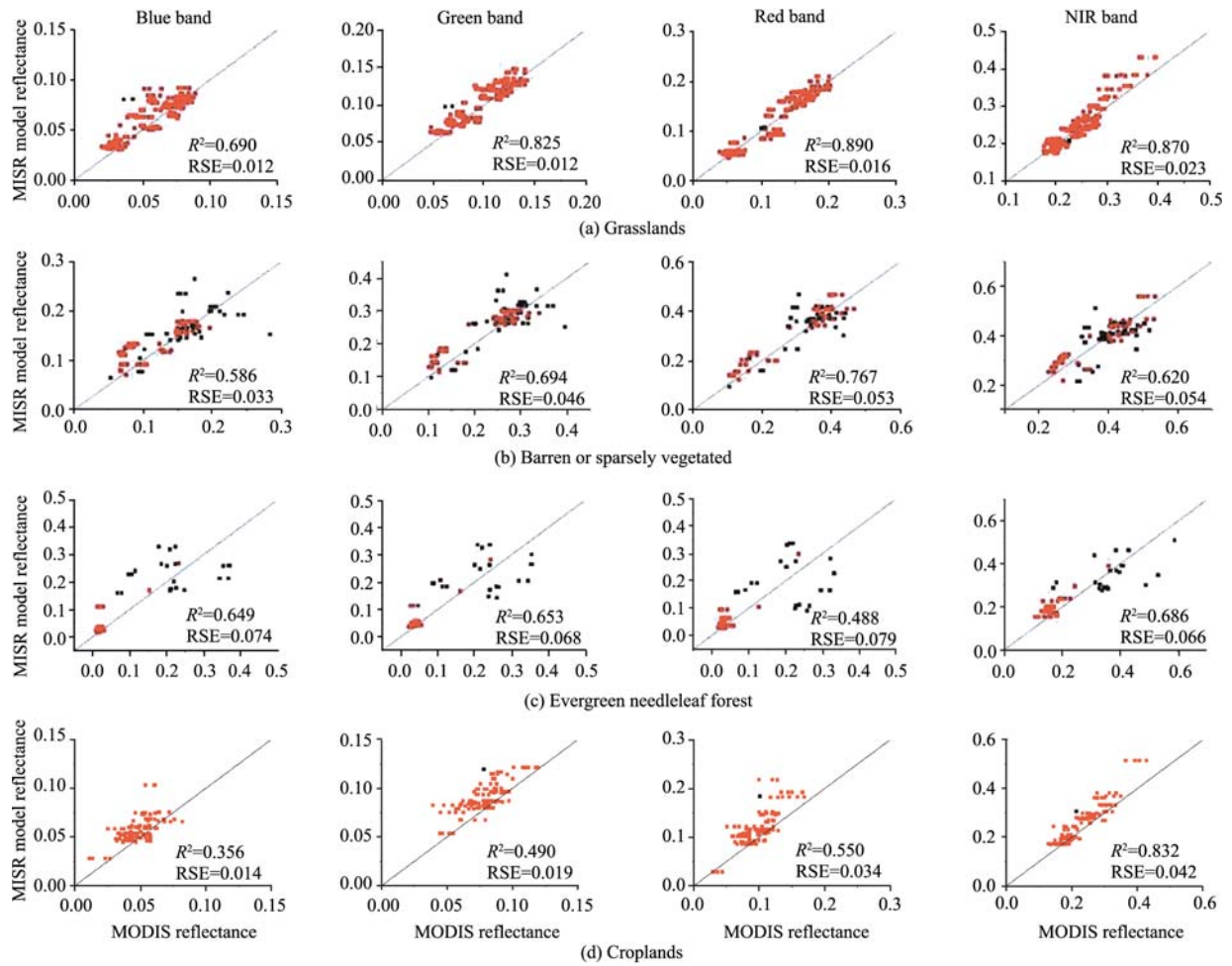


Fig. 2 Fittings of the MISR BRDF model parameters products with the MODIS reflectance products. The red points represent the view zenith angle 30° ; the black points represent the view zenith angle $>30^\circ$. The X coordinate is the MODIS reflectance product (MOD09A1) and the Y coordinate is the reflectance calculated using the MISR BRDF model parameters products.

Table 3 Variability of the extrapolation ability of MODIS BRDF model parameters products with viewing zenith angles

Land cover types	View zenith angle	Blue band		Green band		Red band		NIR band	
		R^2	RSE	R^2	RSE	R^2	RSE	R^2	RSE
Grasslands	30°	0.455	0.017	0.236	0.028	0.495	0.038	0.112	0.061
	$>30^\circ$	0.002	0.037	0.129	0.062	0.002	0.083	0.000	0.120
Barren or sparsely vegetated	30°	0.676	0.023	0.800	0.035	0.855	0.048	0.660	0.063
	$>30^\circ$	0.295	0.040	0.366	0.069	0.557	0.087	0.213	0.100
Evergreen needleleaf forest	30°	0.938	0.031	0.911	0.034	0.908	0.032	0.639	0.053
	$>30^\circ$	0.682	0.065	0.510	0.077	0.545	0.068	0.056	0.127
Croplands	30°	0.155	0.014	0.020	0.022	0.286	0.029	0.368	0.057
	$>30^\circ$	0.031	0.034	0.268	0.053	0.001	0.068	0.000	0.117

Table 4 Variability of the extrapolation ability of MISR BRDF model parameters products with viewing zenith angles

Land cover types	View zenith angle	Blue band		Green band		Red band		NIR band	
		R^2	RSE	R^2	RSE	R^2	RSE	R^2	RSE
Barren or sparsely vegetated	30°	0.688	0.026	0.861	0.033	0.909	0.041	0.820	0.043
	$>30^\circ$	0.409	0.040	0.443	0.057	0.425	0.064	0.238	0.065
Evergreen needleleaf forest	30°	0.757	0.033	0.768	0.030	0.707	0.031	0.724	0.039
	$>30^\circ$	0.065	0.105	0.061	0.096	0.004	0.114	0.231	0.089

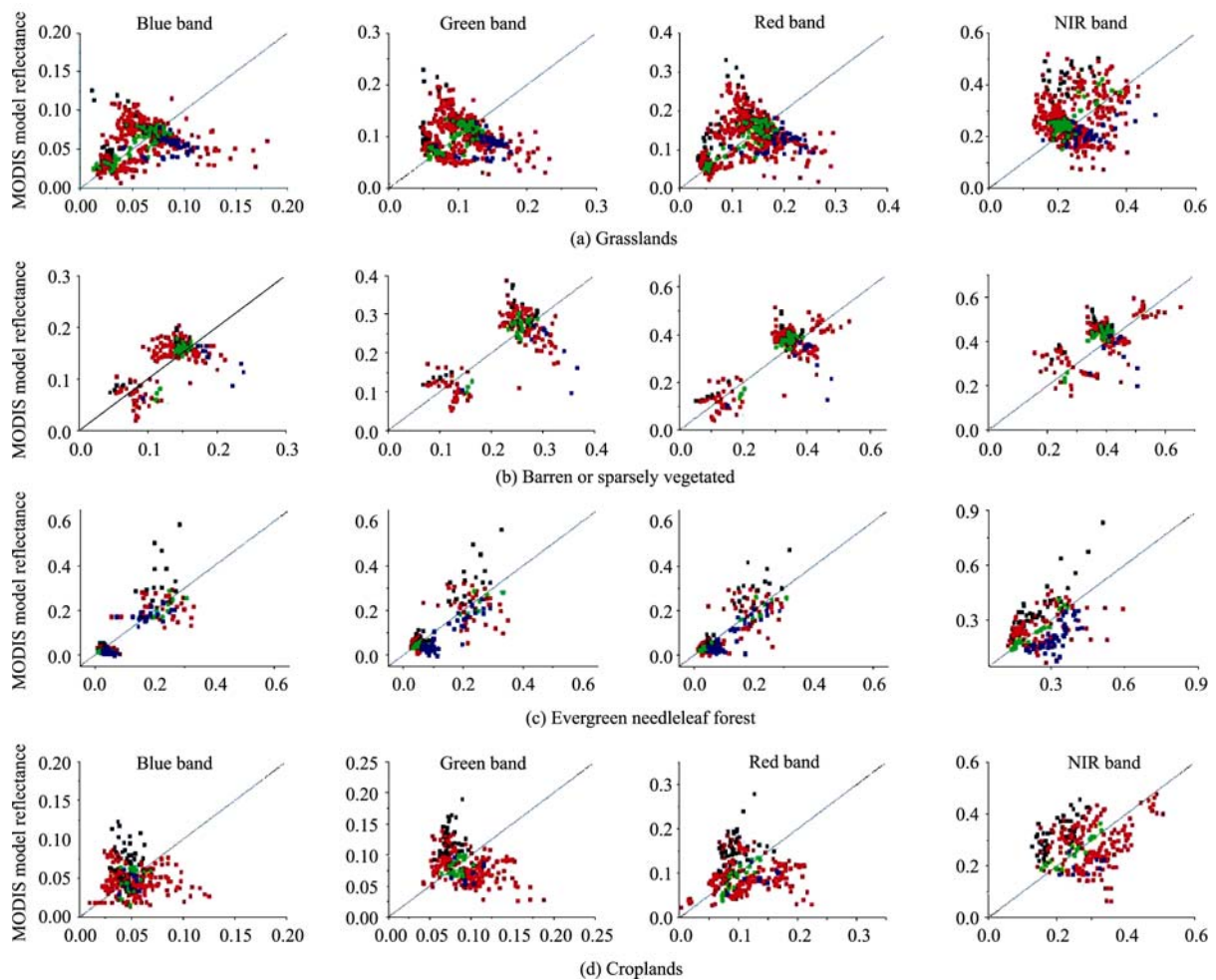


Fig. 3 Fittings of the MODIS BRDF model parameters products with the MISR reflectance product. The black points represent the relative azimuth angle (0°, 30°); the blue points represent the relative azimuth angle (150°, 180°); the green points represent the relative azimuth angle (60°, 120°); and the red points represent the other angles. The X coordinate is the MISR reflectance product and the Y coordinate is the reflectance calculated using the MODIS BRDF model parameters products.

Table 5 Variability of the extrapolation ability of MODIS BRDF model parameters products with relative azimuth angles

Land cover types	*Relative azimuth angle	Blue band		Green band		Red band		NIR band	
		R^2	RSE	R^2	RSE	R^2	RSE	R^2	RSE
Grasslands	CP	0.673	0.012	0.503	0.019	0.722	0.024	0.569	0.043
	PP	0.002	0.039	0.108	0.069	0.001	0.093	0.084	0.151
Barren or sparsely vegetated	CP	0.730	0.021	0.869	0.027	0.901	0.039	0.818	0.052
	PP	0.248	0.049	0.241	0.089	0.366	0.116	0.000	0.127
Evergreen needleleaf forest	CP	0.964	0.026	0.955	0.026	0.948	0.026	0.929	0.024
	PP	0.753	0.069	0.649	0.073	0.683	0.063	0.125	0.124
Croplands	CP	0.195	0.014	0.118	0.013	0.759	0.016	0.838	0.024
	PP	0.000	0.033	0.084	0.050	0.001	0.066	0.041	0.127

* CP represents near cross principal plane, that is the relative azimuth angle $\in (60^\circ, 120^\circ)$, while PP represents near principal plane, that is the relative azimuth angle $\in (0^\circ, 30^\circ)$ or relative azimuth angle $\in (150^\circ, 180^\circ)$

points represent group ④.

The relative azimuth angles of MODIS reflectance products are few in group ①, group ② and group ③, or just belong to one group. So, we did not compare the variability of the extrapolation ability of MISR BRDF model parameters products in the 4 groups.

Similarly, we did the comparison between the extrapolation abilities of MISR BRDF model parameters products on near

principal plane and near cross principal plane (Table 5).

From Fig. 3 we can see that MODIS BRDF model parameters products fit the MISR reflectance product preferably on near cross principal plane (green points), but sparsely on near principal plane (black points and blue points). From Table 5 we can also see that: comparing with the near principal plane, the R^2 increase and the RSE decrease near cross principal plane.

4 RESULTS AND DISCUSSIONS

In this study, we choose MISR and MODIS BRDF model parameters products on the four land cover types which are “Grasslands”, “Barren or sparsely vegetated”, “Evergreen needleleaf forest” and “Croplands” to analyze the extrapolation ability of MISR and MODIS BRDF model parameters products at those directions without viewing data. The research results can provide reference for using MISR and MODIS BRDF model parameters products. For example, when we use the MISR and MODIS BRDF model parameters products to calculate the albedo, we should consider the uncertainty of the reflectance at big view zenith angles that extrapolated by the BRDF model parameters, and possible calculation error.

The results show that: (1) both MODIS and MISR BRDF model parameters products have better extrapolation ability at some viewing directions without measurements. Especially MISR BRDF model parameters products have preferable extrapolation ability at MODIS viewing directions; (2) the extrapolation abilities of both BRDF model parameters products tend to weaken when the viewing zenith angle increases; (3) the extrapolation ability of MODIS BRDF model parameters products is better near cross-principal plane than that near principal plane.

The data used in this study is the MISR and MODIS BRDF model parameters products and reflectance products. It is necessary to know that there is difference between the spatial resolutions of MISR observations at different view zenith angles, while we did not cope with this difference. For the different spatial resolutions of MISR and MODIS, we suppose that the land surface is uniform for large pixel scale. Additionally, there are limitations in obtaining data. For example, the reflectance products of MISR and MODIS used here are not enough to analyze the extrapolation ability of the BRDF model parameters products at all viewing angles. The conclusions in this study are based on finite land cover types. The limitation of the data of different land cover types should be considered if the conclusions are used for other land cover types. After all, the analysis method and the conclusions in this paper are helpful in evaluating the existing BRDF model parameters products and reflectance products at global scale.

Acknowledgements: The authors thank Dr. Fang Hongliang to provide some MISR data for this study.

REFERENCES

Bicheron P and Leroy M. 2000. Bidirectional reflectance distribution function signatures of major biomes observed from space. *Journal of Geophysical Research*, **105**(D21): 26669—26681

- Bull M, Matthews J, Moroney C and Smyth M. 2005. Multi-angle Imaging SpectroRadiometer (MISR) Data Products Specifications. <http://www-misr.jpl.nasa.gov>
- Diner D J, Martonchik J V, Borel C, Gerstl S A W, Gordon H R, Knyazikhin Y, Myneni R, Pinty B and Verstraete M M. 1999. Level 2 Surface Retrieval Algorithm Theoretical Basis. <http://www-misr.jpl.nasa.gov>
- Feng X M and Zhao Y S. 2007. On MSDT inversion with multi-angle remote sensing data. *Science in China Series D: Earth Sciences*, **50**(3): 422—429
- Jiao Z T, Wang J D, Xie L O, Zhang H, Yan G J, He L M and Li X W. 2005. Initial validation of MODIS albedo product by using field measurements and airborne multiangular remote sensing observations. *Journal of Remote Sensing*, **9**(1): 64—72
- Jin Y F, Gao F, Schaaf C B, Li X W, Strahler A H, Bruegge C J and Martonchik J V. 2002. Improving MODIS surface BRDF/Albedo retrieval with MISR multiangle observations. *IEEE Transactions on Geoscience and Remote Sensing*, **40**(7): 1593—1604
- Leroy M and Roujean J L. 1994. Sun and view angle corrections on reflectances derived from NOAA/AVHRR data. *IEEE Transactions on Geoscience and Remote Sensing*, **32**(3): 684—697
- Liang S, Fang H, Chen M, Shuey C J, Walthall C, Daughtry C, Morisette J, Schaaf C and Strahler A. 2002. Validating MODIS land surface reflectance and albedo products: methods and preliminary results. *Remote Sensing of Environment*, **83**(1-2): 149—162
- Lucht W, Schaaf C B and Strahler A H. 2000. An algorithm for the retrieval of albedo from space using semiempirical BRDF models. *IEEE Transactions on Geoscience and Remote Sensing*, **38**(2): 977—998
- Rahman H, Pinty B and Verstraete M M. 1993. Coupled surface-atmosphere reflectance (CSAR) model 2. Semiempirical surface model usable with NOAA advanced very high resolution radiometer data. *Journal of Geophysical Research*, **98**(P): 20791—20801
- Roujean J L, Leroy M and Deschamps P Y. 1992. A bi-directional reflectance model of the Earth's surface for the correction of remote sensing data. *Journal of Geophysical Research*, **97**(D18): 20455—20468
- Schaaf C B, Gao F, Strahler A H, Lucht W, Li X, Tsang T, Strugnell N C, Zhang X, Jin Y, Muller J P, Lewis P, Barnsley M, Hobson P, Disney M, G R, Dunderdale M, Doll C, Entremont R P, Hu B, Liang S, Privette J L and Roy D. 2002. First operational BRDF, albedo nadir reflectance products from MODIS. *Remote Sensing of Environment*, **83**(1): 135—148
- Wan H W, Wang J D, Xiao Z Q, Lin H B and Wang Z S. 2007. Research on MISR data processing method and application. *Remote Sensing Information*, **4**: 16—19
- Wanner W, Strahler A H, Hu B, Lewis P, Muller J-P, Li X, Schaaf B and Barnsley M J. 1997. Global retrieval of bidirectional reflectance and albedo over land from EOS MODIS and MISR data: Theory and algorithm. *Journal of Geophysical Research*, **102**(D14): 17143—17162

MISR 和 MODIS 二向性反射数据产品的对比分析

陈永梅^{1,2}, 王锦地¹, 梁顺林³, 王东伟¹, 马 斌¹

1. 北京师范大学 地理学与遥感科学学院 100875;

2. 解放军理工大学气象学院, 江苏 南京 211101;

3. 美国马里兰大学 地理系 MD20742

摘 要: 利用 4 种地表类型共 16 个地面站点的 MISR 9 个角度反射率数据产品和 MODIS 反射率数据产品 (MOD09A1), 对比两种传感器获取的地表方向反射观测数据和用 BRDF 模型参数产品计算的方向反射数据, 分析了这两种 BRDF 模型参数的外推能力。研究结果表明: (1) MISR 和 MODIS BRDF 模型参数数据产品都具有一定的对观测数据以外方向反射的外推能力, 相比用 MISR BRDF 模型参数数据外推到相应 MODIS 观测角度方向反射的结果一致性较强。(2) 采用两种 BRDF 模型参数推算的方向反射率与观测数据的接近程度有随观测天顶角的增大而减弱的趋势, 在观测天顶角较小时一致性较好。(3) 所用数据处理结果显示, MODIS BRDF 模型参数数据产品在近垂直主平面方向反射率推算结果相比近主平面方向的推算结果更接近观测数据。

关键词: BRDF 模型, MISR, MODIS, 模型参数产品, 外推能力

中图分类号: TP702

文献标识码: A

1 引 言

地表方向反射特性由地物结构和光学特性决定, 常用二向性反射分布函数(BRDF)描述。地表的 BRDF 特征在遥感数据分析和应用中越来越受到重视(Lucht 等, 2000; Wanner 等, 1997)。这是由于根据地表的 BRDF 模型, 可以计算地表半球各方向的反射率, 进而得到更准确的反照率计算数据; 用对地表的多角度观测数据, 可以通过 BRDF 模型反演地表像元结构参数, 如用植被 BRDF 模型反演植被冠层叶面积指数(Feng & Zhao, 2007)。另外 BRDF 模型可以用于将不同观测方向的反射率订正到统一的天顶观测方向上(Leroy & Roujean, 1994; Lucht 等, 2000), 这在多种遥感图像数据融合和时间序列观测数据分析里经常遇到。因此, 现有多角度遥感观测数据产品对地表像元尺度 BRDF 特征的表达、BRDF 模型参数数据产品在相关研究中的适用性, 是数据使用者特别关注的问题。

目前, 多角度成像光谱仪(MISR)和中等分辨率

成像光谱仪(MODIS)数据研究组分别提供有限观测角度的地表反射率数据产品, 同时也分别用多角度观测数据拟合得到 BRDF 模型参数数据产品, 用来外推其他观测方向的反射率, 再对所有半球方向反射率积分计算得到反照率数据产品, 以方便用户的使用。对 BRDF 模型参数数据产品的适用性可以通过对地表反照率的精度验证评价, 前人就 MODIS 反照率产品的验证做过大量的工作(Jiao 等, 2005; Liang 等, 2002)。但是反照率并不一定包含地表二向性反射的完整信息, 相同的反照率可能对应不同的 BRDF 模型参数。因此, 分析 MISR 和 MODIS BRDF 模型参数产品对地表除反射率数据产品中观测方向以外的其他方向反射率的外推能力, 是评价 BRDF 模型参数产品适用性的一个重要方法。要分析 BRDF 模型参数的外推能力, 往往需要大量的地面测量二向反射率数据, 但是多种地类的地面测量二向反射率数据并不容易获得; 另外地面目标的二向反射率多是通过野外测量或航空测量得到的(Bicheron & Leroy, 2000), 即使测量角度足够, 其空间分辨率也

收稿日期: 2008-04-28; 修订日期: 2008-10-31

基金项目: 国家自然科学基金项目(编号: 40571107, 40871163)、国家重点基础研究发展规划项目(973 项目)(编号: 2007CB714407)和国家自然科学基金国际合作与交流项目(编号: 40640420073)。

第一作者简介: 陈永梅(1983—), 女, 2008 年 7 月毕业于北京师范大学地理学与遥感科学学院, 获理学硕士学位, 现工作于南京解放军理工大学气象学院。

通讯作者: 王锦地, E-mail: wangjd@bnu.edu.cn。

不适合用来分析 1.1km 和 1km 分辨率的遥感数据产品。本文利用 MISR 和 MODIS 数据产品的相似性, 对比分析 MISR 和 MODIS BRDF 模型参数数据产品对实际观测方向外的其他方向上反射数据的外推能力。由于 MISR 和 MODIS BRDF 模型参数数据产品和反射率数据产品空间分辨率相似, 且它们前 4 个波段的波长范围相近, 已知 MISR 的 9 个观测角度, 可以用 MODIS BRDF 模型参数数据产品计算这 9 个 MISR 观测角度上的反射率, 通过对比这 9 个角度反射率的计算值与 MISR 观测值, 对 MODIS BRDF 模型参数数据产品的外推能力进行分析。同样, 可以利用 MODIS 反射率数据产品(MOD09A1), 考察 MISR BRDF 模型参数数据产品的外推能力。从分析中得到对两种 BRDF 模型参数数据产品的对比结果。

2 研究所用数据和 BRDF 模型

2.1 典型地类观测站点

本研究所用数据为 2001 年全年的 MISR 和 MODIS BRDF 模型参数数据产品和反射率数据产品。其中 MODIS BRDF 模型参数数据产品和反射率数据产品下载自 ORNL DAAC(Oak Ridge National Laboratory Distributed Active Archive Center), MISR BRDF 模型参数数据产品和反射率数据产品由马里兰大学 Fang Hongliang 博士提供。地表类别包括草地(grasslands)、荒地或稀疏植被地表(barren or sparsely vegetated)、长绿针叶林(evergreen needleleaf forest)和农作物(croplands)4 种地表类型共 16 个站点, 每种地表类型所属的站点信息如表 1。

2.2 MISR 反射率数据产品和 BRDF 模型参数数据产品

MISR 是搭载在极轨卫星 Terra 上的传感器, 可从 9 个方向分 4 个波段对地观测。其 9 个观测角度分别为 0° , $\pm 26.1^\circ$, $\pm 45.6^\circ$, $\pm 60.0^\circ$ 和 $\pm 70.5^\circ$; 4 个波段分布在可见光到近红外光谱范围内, 其中心波长分别为 446, 558, 672 及 867nm(Bull 等, 2005)。本文所选用的 MISR 数据为经系统辐射纠正、几何纠正和大气纠正环进行大气纠正的二级产品——MISR 9 个观测角度地表反射率数据产品, 和用这 9 个角度反射率数据所拟合得到的 MISR BRDF 模型参数数据产品, 二者空间分辨率均为 1.1km(Diner 等, 1999; Wan 等, 2007)。

MISR BRDF 模型参数产品生成所用的 BRDF 模型为改进的 Rahman 模型, 模型表达式如下(Diner

表 1 不同地表类型所属地面站点的名称和经纬度信息

类别	站点名称	经度	纬度
草地	Sevilleta BigFoot	106.70°W	34.36°N
	Konza Prairie LTER	96.56°W	39.08°N
	Rannells Ranch (grazed)	96.53°W	39.14°N
	Sevilleta Nat Refuge-Mackenzie Flats	106.67°W	34.36°N
荒地或稀疏植被	La Paz	110.44°W	24.13°N
	Arabia1	46.76°E	18.88°N
	Ivanpah Playa Nevada/California	115.39°W	35.55°N
	Railroad Valley Playa 2	115.70°W	38.50°N
长绿针叶林	Sask.-1994 Harv. Jack Pine	104.66°W	53.91°N
	BOREAS NSA-Old Black Spruce	98.48°W	55.88°N
	BOREAS NSA Young Jack Pine	98.29°W	55.90°N
	Black Hills	103.65°W	44.16°N
农作物	Bondville	88.29°W	40.01°N
	Pleasant Plains	89.88°W	39.50°N
	Walnut River Watershed	96.86°W	37.52°N
	ARM Southern Great Plains site-Lamont	97.49°W	36.61°N

等, 1999; Rahman 等, 1993):

$$R_{\text{model}}(-\mu, \mu_0, \phi) = r_0 \times \frac{\mu^{k-1} \mu_0^{k-1}}{(\mu + \mu_0)^{1-k}} \times \exp[bp(\Omega)] \times h(-\mu, \mu_0, \phi) \quad (1)$$

式中, r_0 , k , b 为 3 个模型常数, μ 和 μ_0 分别为观测天顶角 θ 和太阳天顶角 ϑ 的余弦值, ϕ 为相对方位角。函数 $p(\Omega)$ 为散射角 Ω 的函数, 在此处定义为 θ , ϑ 和 ϕ 的函数:

$$p(\Omega) = \cos \Omega = -\mu \mu_0 + (1 - \mu^2)^{1/2} \times (1 - \mu_0^2)^{1/2} \times \cos \phi \quad (2)$$

式中, 函数 h 为代表热点的函数, 表示为:

$$h(-\mu, \mu_0, \phi) = 1 + \frac{1 - r_0}{1 + G(-\mu, \mu_0, \phi)} \quad (3)$$

式中, G 是观测天顶角, 太阳天顶角和相对方位角的函数:

$$G(-\mu, \mu_0, \phi) = \{(\mu^{-2} - 1) + (\mu_0^{-2} - 1) + 2 \left[\sqrt{(\mu^{-2} - 1)(\mu_0^{-2} - 1)} \right] \cos \phi\}^{1/2} \quad (4)$$

由式(1)–(4)可知, 若已知 Rahman 模型的 3 个参数(r_0 , k , b), 可代入式(1) 计算任意观测角度(θ , ϑ , ϕ)上的反射率。MISR BRDF 模型参数数据产品即为空间分辨率为 1.1km 的 Rahman 模型的 3 个参数(r_0 , k , b)。

2.3 MODIS 反射率数据产品和 BRDF 模型参数数据产品

MODIS 也是搭载在 Terra 卫星上的传感器, 所

用的 MODIS 数据为 MODIS 前 4 个波段的 BRDF 模型参数数据产品(MOD43B1), 空间分辨率为 1km; 以及 MODIS 反射率产品中空间分辨率为 500m 的产品(MOD09A1)(Schaaf 等, 2002)。

MODIS BRDF 模型参数数据生成所用的 BRDF 模型为半经验的核驱动模型(Lucht 等, 2000; Roujean 等, 1992; Schaaf 等, 2002), 表达式如下:

$$R(\theta, \vartheta, \phi) = f_{\text{iso}} + f_{\text{geo}} K_{\text{geo}}(\theta, \vartheta, \phi) + f_{\text{vol}} K_{\text{vol}}(\theta, \vartheta, \phi) \quad (5)$$

式中, f_{iso} 是一个表示各向同性散射的系数, K_{geo} 和 K_{vol} 是观测天顶角 θ 、太阳天顶角 ϑ 和相对方位角 ϕ 的函数, 分别代表几何光学和体散射分量, f_{geo} 和 f_{vol} 两个系数分别为几何光学和体散射分量的权重。

MODIS 为宽视场对地观测, 主要是通过扫描带的重叠获得多角度观测数据。MODIS BRDF 模型算法以 16d 为周期利用经过大气纠正的地表多角度观测数据对核驱动模型参数进行反演, 得到空间分辨率为 1km 的全球范围内的 BRDF 模型参数数据产品($f_{\text{iso}}, f_{\text{geo}}, f_{\text{vol}}$)。由于 K_{geo} 和 K_{vol} 是 θ, ϑ 和 ϕ 的函数, 由式(5)可知, 若已知 MODIS 核驱动模型的 3 个参数($f_{\text{iso}}, f_{\text{geo}}, f_{\text{vol}}$)可代入式(5)计算任意观测角度(θ, ϑ, ϕ)上的反射率。我们将这个从有限方向观测数据计算其他方向反射率的过程称为模型外推过程。MODIS BRDF 模型参数数据产品即为空间分辨率为 1km 的核驱动模型的 3 个参数($f_{\text{iso}}, f_{\text{geo}}, f_{\text{vol}}$)。

3 研究方法和结果

3.1 MISR 和 MODIS 像元数据产品在空间、时间和波谱上的对应

在对 MISR 和 MODIS 数据产品进行分析处理前, 需要建立两种传感器数据产品在空间、时间和波谱上的对应关系。

ORNL DAAC 提供的典型地面站点所对应的 MODIS 像元的数据产品以及站点经纬度信息, 利用通用投影转换包(general cartographic transformation package software), 根据每个站点的经纬度坐标可以找到每个站点所对应的 MODIS 像元和 MISR 像元。MISR 反射率产品空间分辨率为 1.1km, MODIS BRDF 模型参数数据产品空间分辨率为 1km, 二者差别较小, 因此二者在空间位置上可以近似认为直接相互对应。本文采用站点的 MODIS 反射率数据产品(MOD09A1)空间分辨率为 500m, 而 MISR BRDF 模型参数数据产品的空间分辨率为 1.1km, 一个 MISR BRDF 模型参数数据产品像元对应大约 4 个 MOD09A1 像元, 由于此 MODIS 反射率数据为

8d 内最好的反射率, 因此这 4 个像元的成像时间以及观测角度可能不同, 在假定站点地表在 1km 范围内均一、且其像元的方向反射特性在 8d 内近似不变的情况下, 可以把这 4 个像元的反射率数据看作是对一个 MISR 像元的 4 个不同角度的观测。这样, 就建立 MISR BRDF 模型参数数据产品和 MODIS 反射率数据产品的空间对应关系。

由于 MISR 为 9 个角度准同步对地观测, MISR BRDF 模型参数数据产品即由 9 个角度瞬时观测数据生成。而 MODIS BRDF 模型参数数据产品则是利用多天的多角度观测和半经验核驱动模型(AMBRALS)反演得到以 16d 为周期的产品, MODIS 反射率产品(MOD09A1)为 8d 一个周期。因此在本研究中, 以 16d 为周期, 对 MISR 9 个角度反射率观测数据和用 MODIS BRDF 模型参数外推到 MISR 这 9 个观测角度的反射率进行比较分析, 即对 16d 内的 MISR 反射率与使用第 1 天 MODIS BRDF 模型参数外推得到的对应于 MISR 9 个角度的反射率进行对比, 依次类推。同样的道理, 以 8d 为周期, 比较分析 MODIS 多角度观测数据和用 MISR BRDF 模型参数外推到 MODIS 观测角度反射率的异同。

MISR 和 MODIS 前 4 个波段是窄波段, 并且两种传感器在可见光和近红外波段非常相似(Jin 等, 2002)。如表 2, MISR 的第 1, 2, 3, 4 波段分别为蓝、绿、红和近红外波段; 可以看作和 MODIS 第 3, 4, 1, 2 波段分别对应。

表 2 MISR 和 MODIS 波段对应信息

波段名	MODIS		MISR	
	波段号	波长/nm	波段号	波长/nm
蓝	3	459—479	1	425—467
绿	4	545—565	2	543—572
红	1	620—670	3	661—683
近红外	2	841—876	4	847—886

3.2 MISR 和 MODIS BRDF 模型参数数据产品的对比分析

对于每个站点像元, 读取相应的 MISR 和 MODIS 像元的 BRDF 模型参数数据产品和多角度反射率数据产品以及相应的入射-观测几何(太阳天顶角, 观测天顶角, 相对方位角)。利用 MISR 9 个角度的入射-观测几何以及 MODIS BRDF 模型参数数据产品所提供的核驱动模型的 3 个核系数可以计算得

到相应的 MISR 9 个角度上的反射率, 将这 9 个角度计算反射率与 MISR 观测反射率数据进行对比, 采用相关系数(R^2)和均方根误差(RSE)考察 MODIS BRDF 模型参数数据产品与 MISR 观测角度上方向反射的接近程度。同样, 已知站点像元 MOD09A1 4 个观测角度的入射-观测几何, 利用 MISR BRDF 模型参数数据产品计算得到 MOD09A1 4 个观测角度上的反射率, 通过比较这 4 个角度的计算反射率与 MOD09A1 观测反射率, 分析 MISR BRDF 模型参数数据产品的外推能力。

3.2.1 两种 BRDF 模型参数数据产品的外推能力随观测天顶角的变化

为了分析两种 BRDF 模型参数数据产品的外推能力随观测天顶角的变化, 将 MISR 和 MODIS 反射

率产品按照观测天顶角分为 2 类: 观测天顶角 30° ; 观测天顶角 $> 30^\circ$ 。

图 1 和图 2 为用两种模型参数产品外推方向反射结果的对比图。图中红色点代表第 1 类, 黑色点代表第 2 类, 所标注波段为 MISR 波段编号。

为了定量分析两种 BRDF 模型参数数据产品的外推能力随观测天顶角的变化, 对用两种 BRDF 模型参数的外推结果, 在大观测天顶角和小观测天顶角两种情况下分别计算了 R^2 和 RSE, 对比结果见表 3 和表 4。由于草地和农作物两种地表类型的 MODIS 反射率数据观测天顶角小于 30° , 因此在表 4 中未做比较。

从图 1 可以看出: MODIS BRDF 模型参数数据产品对 MISR 反射率产品拟合结果在观测天顶角较

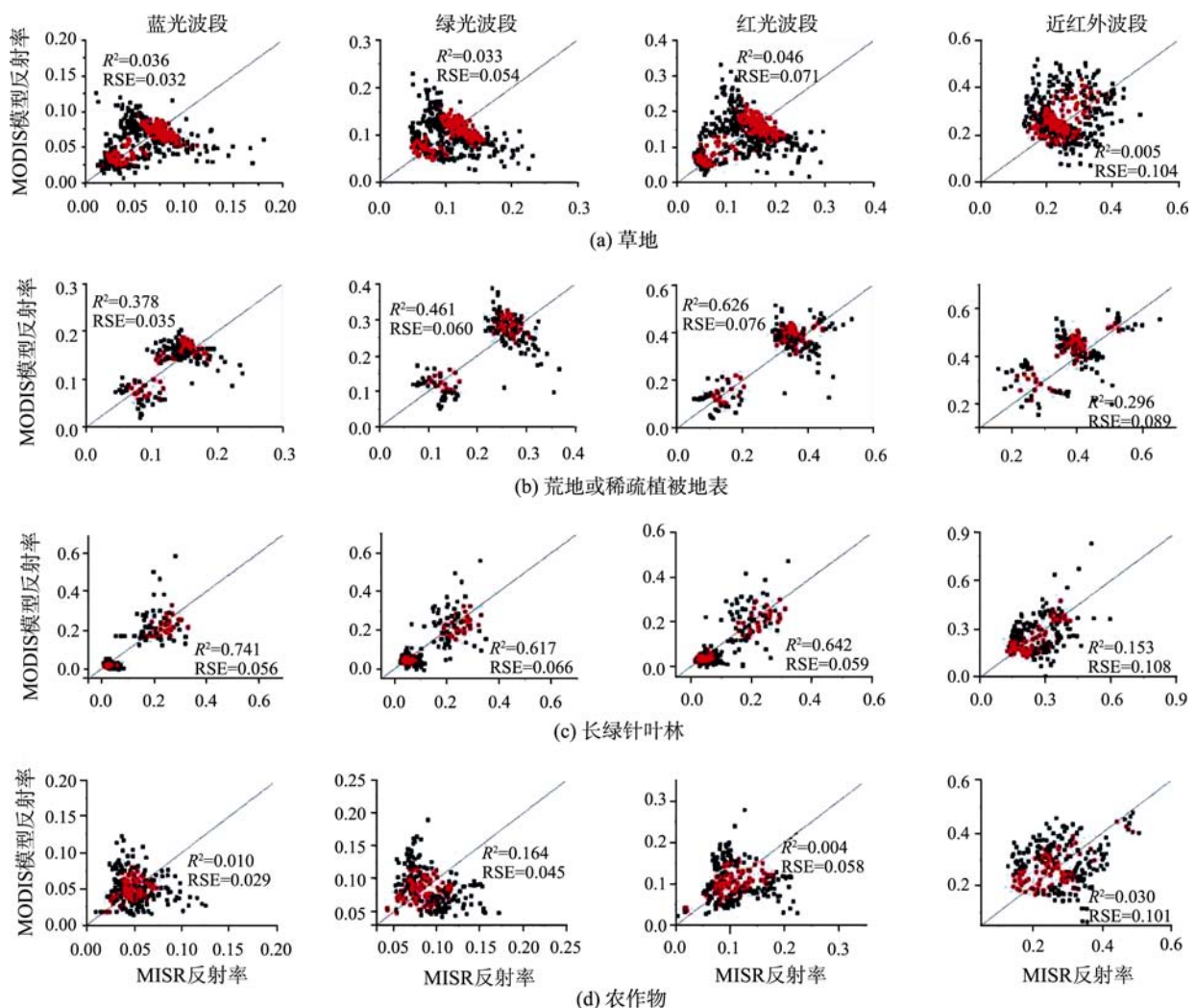


图 1 2001 年 MODIS BRDF 模型参数数据产品对 MISR 9 个角度反射率产品的拟合图

反射率数据产品按照观测天顶角可分为 2 类: 观测天顶角 $< 30^\circ$ 的观测; 观测天顶角 $> 30^\circ$ 的观测; 图中红色代表第 1 类, 黑色代表第 2 类。横坐标为 MISR 反射率数据产品, 纵坐标为利用 MODIS BRDF 模型参数数据产品外推计算出来的 MISR 观测方向的反射率

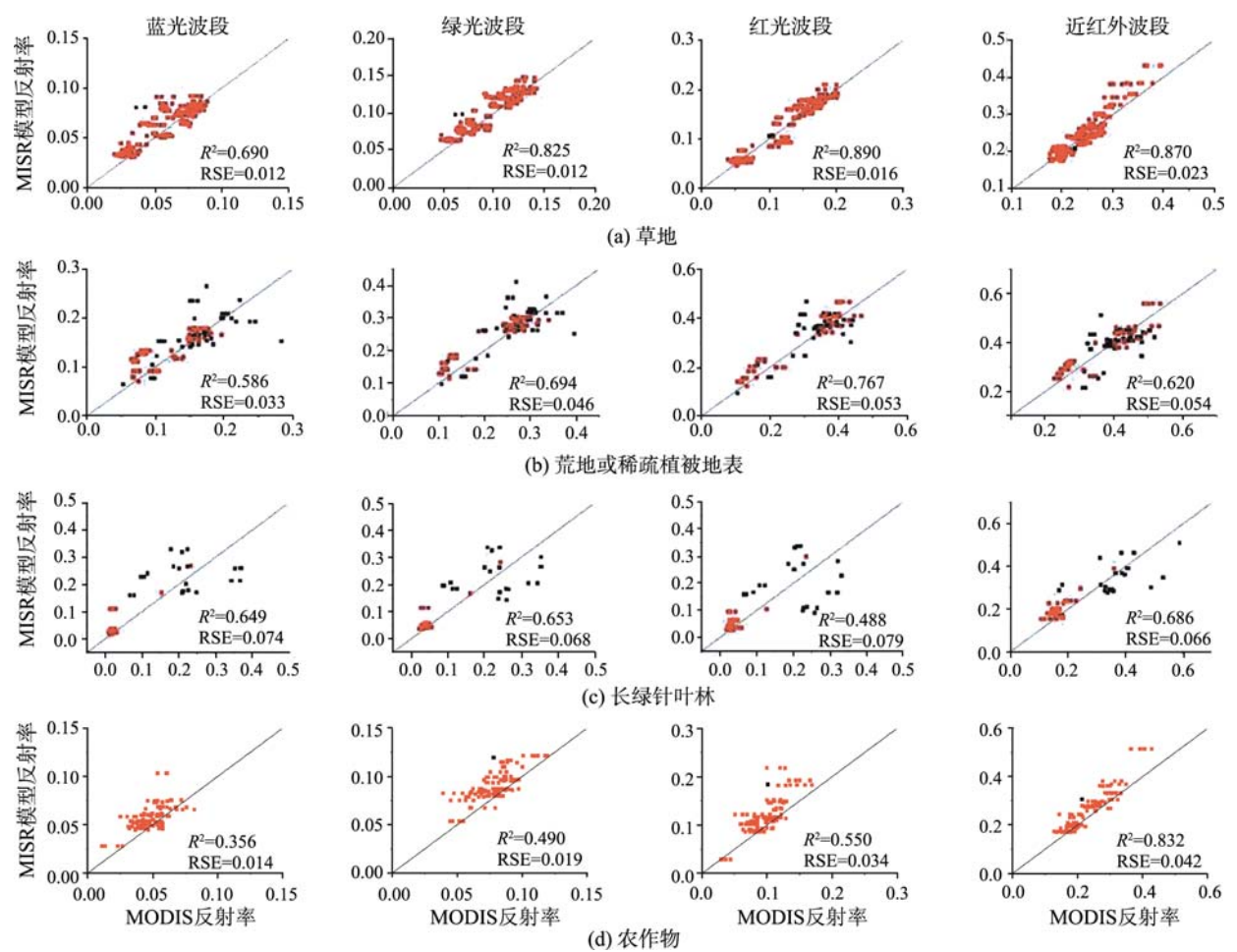


图 2 2001 年 MISR BRDF 模型参数数据产品对 MODIS 反射率产品的拟合图

反射率数据产品按照观测天顶角可分为 2 类: 观测天顶角 $\leq 30^\circ$ 的观测; 观测天顶角 $>30^\circ$ 的观测; 图中红色代表第 1 类, 黑色代表第 2 类。横坐标为 MODIS 反射率数据产品(MOD09A1), 纵坐标为利用 MISR BRDF 模型参数数据产品外推计算出来的 MODIS 观测方向的反射率

表 3 MODIS BRDF 模型参数数据产品对 MISR 反射率数据产品拟合程度与观测天顶角的关系

类别	观测天顶角	蓝光波段		绿光波段		红光波段		近红外波段	
		R^2	RSE	R^2	RSE	R^2	RSE	R^2	RSE
草地	30°	0.455	0.017	0.236	0.028	0.495	0.038	0.112	0.061
	$>30^\circ$	0.002	0.037	0.129	0.062	0.002	0.083	0.000	0.120
荒地或 稀疏植被	30°	0.676	0.023	0.800	0.035	0.855	0.048	0.660	0.063
	$>30^\circ$	0.295	0.040	0.366	0.069	0.557	0.087	0.213	0.100
长绿 针叶林	30°	0.938	0.031	0.911	0.034	0.908	0.032	0.639	0.053
	$>30^\circ$	0.682	0.065	0.510	0.077	0.545	0.068	0.056	0.127
农作物	30°	0.155	0.014	0.020	0.022	0.286	0.029	0.368	0.057
	$>30^\circ$	0.031	0.034	0.268	0.053	0.001	0.068	0.000	0.117

表 4 MISR BRDF 模型参数数据产品对 MODIS 反射率数据产品(MOD09A1)拟合程度与观测天顶角的关系

类别	观测天顶角	蓝光波段		绿光波段		红光波段		近红外波段	
		R^2	RSE	R^2	RSE	R^2	RSE	R^2	RSE
荒地或 稀疏植被	30°	0.688	0.026	0.861	0.033	0.909	0.041	0.820	0.043
	$>30^\circ$	0.409	0.040	0.443	0.057	0.425	0.064	0.238	0.065
长绿 针叶林	30°	0.757	0.033	0.768	0.030	0.707	0.031	0.724	0.039
	$>30^\circ$	0.065	0.105	0.061	0.096	0.004	0.114	0.231	0.089

大时较离散(黑色点),而在观测天顶角较小时拟合结果较好(红色点)。从表3中也可以看出类似的情况:观测天顶角小于 30° 时的拟合结果与观测天顶角大于 30° 时的结果相比, R^2 普遍增大,RSE普遍减小。

从图2和表4中可以看出:由于MISR可准同时获取同一地面目标9个观测角度的观测数据,与MODIS利用多轨重叠获取多角度观测数据的方式相比,具有获取更为丰富的观测角度信息、特别是大天顶角观测信息的优势,因而MISR BRDF模型参数数据产品对MODIS反射率产品拟合结果总体较好,MISR BRDF模型参数数据产品的外推能力也更好些,虽然也有在观测天顶角增大时拟合结果离散性增加的趋势。这点也可从图1和图2草地类和农作物地类的结果对比中明确看到。

3.2.2 MODIS BRDF 模型参数数据产品的外推能力随相对方位角的变化

为了分析两种BRDF模型参数数据产品的外推能力随太阳入照方向和观测方向之间的相对方位角的变化,将MISR和MODIS反射率产品按照相对方位角分为4类:相对方位角($0^\circ, 30^\circ$); 相对方位角($150^\circ, 180^\circ$); 相对方位角($60^\circ, 120^\circ$); 其他相对方位角度观测。

图3为用MODIS模型参数产品外推结果与相应方向反射观测值的对比图。图中黑色点代表第1类,蓝色点代表第2类,绿色点代表第3类,红色点代表第4类。

由于MODIS反射率数据在第1类、第2类、第

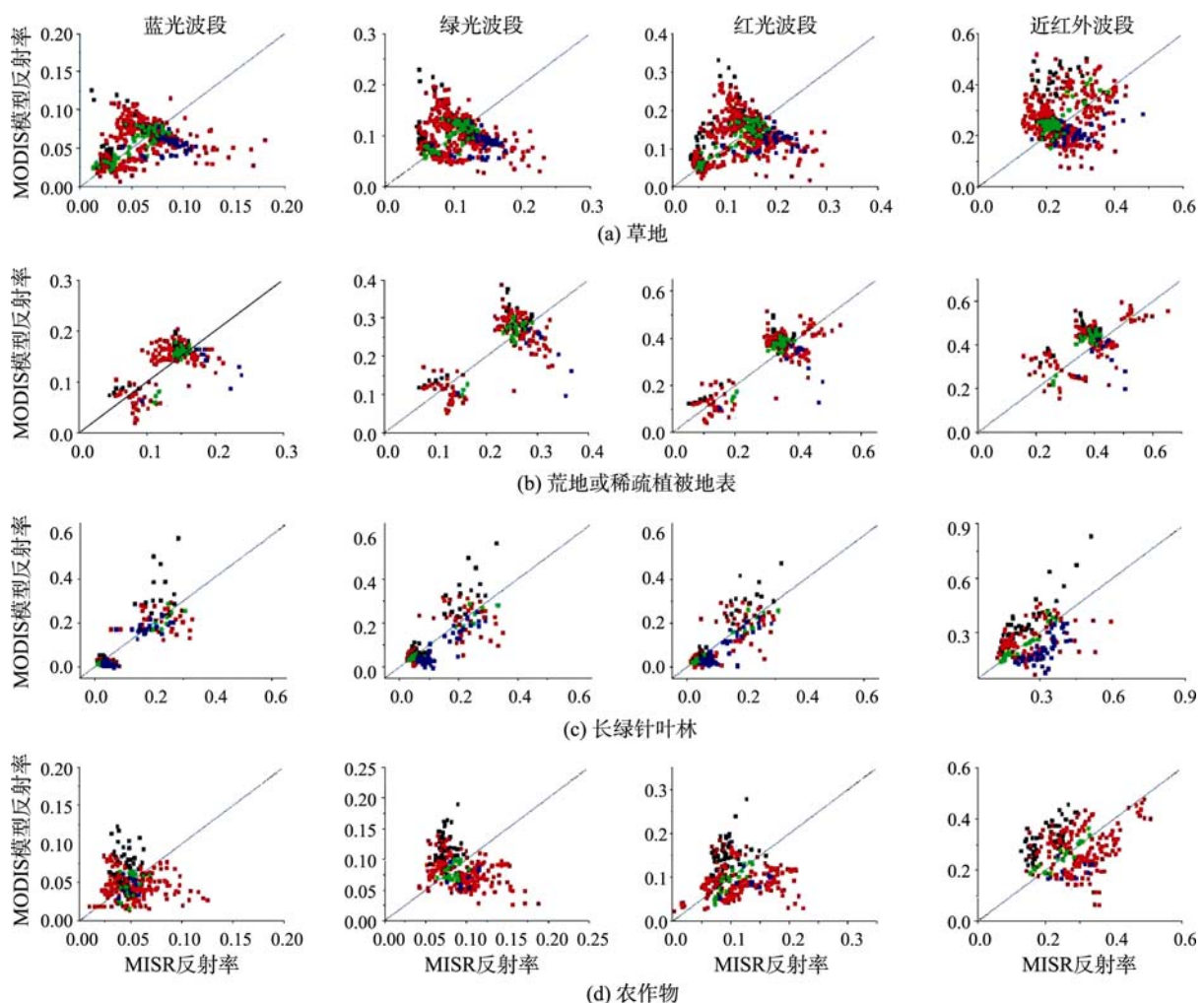


图3 2001年MODIS BRDF模型参数数据产品对MISR 9个角度反射率产品的拟合图

反射率数据产品按照相对方位角分为4类: 相对方位角($0^\circ, 30^\circ$); 相对方位角($150^\circ, 180^\circ$); 相对方位角($60^\circ, 120^\circ$); 其他相对方位角度观测; 图中黑色代表第1类,蓝色代表第2类,绿色代表第3类,红色代表第4类。横坐标为MISR反射率数据产品,纵坐标为利用MODIS BRDF模型参数数据产品外推计算出来的MISR观测方向的反射率

表 5 MODIS BRDF 模型参数数据产品对 MISR 反射率数据产品拟合程度与相对方位角的关系

IGBP 类别	*相对方位角	蓝光波段		绿光波段		红光波段		近红外波段	
		R^2	RSE	R^2	RSE	R^2	RSE	R^2	RSE
草地	CP	0.673	0.012	0.503	0.019	0.722	0.024	0.569	0.043
	PP	0.002	0.039	0.108	0.069	0.001	0.093	0.084	0.151
荒地或稀疏植被	CP	0.730	0.021	0.869	0.027	0.901	0.039	0.818	0.052
	PP	0.248	0.049	0.241	0.089	0.366	0.116	0.000	0.127
长绿针叶林	CP	0.964	0.026	0.955	0.026	0.948	0.026	0.929	0.024
	PP	0.753	0.069	0.649	0.073	0.683	0.063	0.125	0.124
农作物	CP	0.195	0.014	0.118	0.013	0.759	0.016	0.838	0.024
	PP	0.000	0.033	0.084	0.050	0.001	0.066	0.041	0.127

*表中 CP 表示近垂直主平面观测方向, 即相对方位角 (60°, 120°), PP 表示近主平面观测方向, 即相对方位角 (0°, 30°)或相对方位角 (150°, 180°)

类的点很少, 或者只属于其中某一类, 对比性不强, 因此未做 MISR BRDF 模型参数数据产品的外推能力在这 4 种情况的对比。

类似地, 分别做了 MODIS BRDF 模型参数数据产品的外推能力在近主平面(第 类和第 类)与近垂直主平面(第 类)两种情况的对比(表 5)。

从图 3 中可以看到: MODIS BRDF 模型参数数据产品对 MISR 反射率产品拟合结果在近垂直主平面较好(绿色点), 而在近主平面方向较离散(黑色点和蓝色点)。从表 5 中也可以看出, 近垂直主平面方向的拟合结果与近主平面方向的拟合结果相比, R^2 普遍增大, RSE 普遍减小。

4 结论和讨论

本文用 MISR 和 MODIS 反射率产品分别对草地、荒地或稀疏植被地表、长绿针叶林以及农作物 4 种地表类型的 MODIS 和 MISR BRDF 模型参数数据产品, 分析比较了在除观测方向以外的其他方向上的模型外推计算值和观测数据, 所得到的结论为 MISR 和 MODIS BRDF 模型参数数据产品的使用者提供了必要的参考。例如, 当采用 MISR 和 MODIS BRDF 模型参数产品计算地表反照率时, 需要考虑用模型参数外推到大天顶角方向反射数据的不确定性, 及其可能引起的反照率计算误差。

研究结果表明: (1)MISR 和 MODIS BRDF 模型参数数据产品对观测方向以外的其他方向反射率有一定的外推能力, 用 MISR BRDF 模型参数在相应的 MODIS 观测角度上的外推计算结果与观测数据更接近。(2)采用两种 BRDF 模型参数推算的方向反射率与观测数据的接近程度随观测天顶角的增大而减弱的趋势, 在观测天顶角较小时一致性较好。

(3)MODIS BRDF 模型参数数据产品在近垂直主平面方向反射率推算结果相比近主平面方向的推算结果更接近观测数据。

需要说明的是, 本研究仅采用数据网站提供的站点 MISR 和 MODIS BRDF 数据产品, 并没有对 MISR 多角度数据获取中不同天顶角观测的空间分辨率差异做更多的处理。对于 MISR 和 MODIS 像元数据产品的空间分辨率差异, 也采用了相对大像元尺度地表均一的假定。另外, 在获取数据方面还存在一些局限性。如, 采用 MISR 和 MODIS 反射率产品的观测角度有限, 还不足以对 BRDF 模型参数数据产品在所有观测角度上的外推结果做完整的分析评价。由于现有的结论仅依据已有站点的典型地类的观测数据, 当将本文的结论用到其他地类时, 需要考虑站点获取数据的有限性。但是本文提出的对比验证方法和结果, 对进一步评价现有全球尺度的 BRDF 模型参数和方向反射数据产品, 具有参考价值。

致谢: 感谢方红亮博士提供本文工作所用 MISR 数据。

REFERENCES

- Bicheron P and Leroy M. 2000. Bidirectional reflectance distribution function signatures of major biomes observed from space. *Journal of Geophysical Research*, **105**(D21): 26669—26681
- Bull M, Matthews J, Moroney C and Smyth M. 2005. Multi-angle Imaging SpectroRadiometer (MISR) Data Products Specifications. <http://www-misr.jpl.nasa.gov>
- Diner D J, Martonchik J V, Borel C, Gerstl S A W, Gordon H R, Knyazikhin Y, Myneni R, Pinty B and Verstraete M M. 1999. Level 2 Surface Retrieval Algorithm Theoretical Basis.

<http://www-misr.jpl.nasa.gov>

- Feng X M and Zhao Y S. 2007. On MSDT inversion with multi-angle remote sensing data. *Science in China Series D: Earth Sciences*, **50**(3): 422—429
- Jiao Z T, Wang J D, Xie L O, Zhang H, Yan G J, He L M and Li X W. 2005. Initial validation of MODIS albedo product by using field measurements and airborne multiangular remote sensing observations. *Journal of Remote Sensing*, **9**(1): 64—72
- Jin Y F, Gao F, Schaaf C B, Li X W, Strahler A H, Bruegge C J and Martonchik J V. 2002. Improving MODIS surface BRDF/Albedo retrieval with MISR multiangle observations. *IEEE Transactions on Geoscience and Remote Sensing*, **40**(7): 1593—1604
- Leroy M and Roujean J L. 1994. Sun and view angle corrections on reflectances derived from NOAA/AVHRR data. *IEEE Transactions on Geoscience and Remote Sensing*, **32**(3): 684—697
- Liang S, Fang H, Chen M, Shuey C J, Walthall C, Daughtry C, Morisette J, Schaaf C and Strahler A. 2002. Validating MODIS land surface reflectance and albedo products: methods and preliminary results. *Remote Sensing of Environment*, **83**(1-2): 149—162
- Lucht W, Schaaf C B and Strahler A H. 2000. An algorithm for the retrieval of albedo from space using semiempirical BRDF models. *IEEE Transactions on Geoscience and Remote Sensing*, **38**(2): 977—998
- Rahman H, Pinty B and Verstraete M M. 1993. Coupled surface-atmosphere reflectance (CSAR) model 2. Semiempirical surface model usable with NOAA advanced very high resolution radiometer data. *Journal of Geophysical Research*, **98**(P): 20791—20801
- Roujean J L, Leroy M and Deschamps P Y. 1992. A bi-directional reflectance model of the Earth's surface for the correction of remote sensing data. *Journal of Geophysical Research*, **97**(D18): 20455—20468
- Schaaf C B, Gao F, Strahler A H, Lucht W, Li X, Tsang T, Strugnell N C, Zhang X, Jin Y, Muller J P, Lewis P, Barnsley M, Hobson P, Disney M, G. R, Dunderdale M, Doll C, Entremont R P, Hu B, Liang S, Privette J L and Roy D. 2002. First operational BRDF, albedo nadir reflectance products from MODIS. *Remote Sensing of Environment*, **83**(1): 135—148
- Wan H W, Wang J D, Xiao Z Q, Lin H B and Wang Z S. 2007. Research on MISR data processing method and application. *Remote Sensing Information*, **4**: 16—19
- Wanner W, Strahler A H, Hu B, Lewis P, Muller J-P, Li X, Schaaf B and Barnsley M J. 1997. Global retrieval of bidirectional reflectance and albedo over land from EOS MODIS and MISR data: Theory and algorithm. *Journal of Geophysical Research*, **102**(D14): 17143—17162

附中文参考文献

- 焦子锴, 王锦地, 谢里欧, 张颢, 阎广建, 何立明, 李小红. 地面和机载多角度观测数据的反照率反演及对 MODIS 反照率产品的初步验证. *遥感学报*, 2005, **9**(1): 64—72
- 万华伟, 王锦地, 肖志强, 林皓波, 王镭森. MISR 多角度遥感数据的组件库处理方法及数据分析. *遥感信息*, 2007, **4**: 16—19